
eXponential FAmily Dynamical Systems (XFADS): Large-scale nonlinear Gaussian state-space modeling

Matthew Dowling

Champalimaud Foundation, Portugal
New York University, New York, USA
md6276@nyu.edu

Yuan Zhao

National Institute of Mental Health, USA
yuan.zhao@nih.gov

Il Memming Park

Champalimaud Foundation, Portugal
memming.park@research.fchampalimaud.org

Abstract

State-space graphical models and the variational autoencoder framework provide a principled apparatus for learning dynamical systems from data. State-of-the-art probabilistic approaches are often able to scale to large problems at the cost of flexibility of the variational posterior or expressivity of the dynamics model. However, those consolidations can be detrimental if the ultimate goal is to learn a generative model capable of explaining the spatiotemporal structure of the data and making accurate forecasts. We introduce a low-rank structured variational autoencoding framework for nonlinear Gaussian state-space graphical models capable of capturing dense covariance structures that are important for learning dynamical systems with predictive capabilities. Our inference algorithm exploits the covariance structures that arise naturally from sample based approximate Gaussian message passing and low-rank amortized posterior updates – effectively performing approximate variational smoothing with time complexity scaling linearly in the state dimensionality. In comparisons with other deep state-space model architectures our approach consistently demonstrates the ability to learn a more predictive generative model. Furthermore, when applied to neural physiological recordings, our approach is able to learn a dynamical system capable of forecasting population spiking and behavioral correlates from a small portion of single trials.

1 Introduction

State-space models (SSM) are invaluable for understanding the temporal structure of complex natural phenomena through their underlying dynamics^{1–3}. While engineering or physics problems often assume the dynamical laws of the system of interest are known to a high degree of accuracy, in an unsupervised data-driven investigation, they have to be learned from the observed data. The variational autoencoder (VAE) framework makes it possible to jointly learn the parameters of the state-space description and an inference network to amortize posterior computation of the unknown latent state^{4–7}. However, it can be challenging to structure the variational approximation and design an inference network that permits fast evaluation of the loss function (evidence lower bound or ELBO) while preserving the temporal structure of the posterior.

In this work, we develop a structured variational approximation, approximate ELBO, and inference network architecture for generative models specified by nonlinear dynamical systems with Gaussian state noise. Our main contributions are as follows,

- (i) A structured amortized variational approximation that combines the prior dynamics with low-rank data updates to parameterize Gaussian distributions with dense covariance matrices,
- (ii) Conceptualizing the approximate smoothing problem as an approximate filtering problem for pseudo-observations that encode a representation of current and future data, and,
- (iii) An inference algorithm that scales $\mathcal{O}(TL(Sr + S^2 + r^2))$ – made possible by exploiting the low-rank structure of the amortization network as well as Monte Carlo integration of the latent state through the dynamics.

2 Background

State-space models are probabilistic graphical models where observations \mathbf{y}_t in discrete time are conditionally independent given a continuous latent state, \mathbf{z}_t , evolving according to Markovian dynamics, so that the complete data likelihood for T consecutive observations factorizes as,

$$p(\mathbf{y}_{1:T}, \mathbf{z}_{1:T}) = p_{\theta}(\mathbf{z}_1) p_{\psi}(\mathbf{y}_1 | \mathbf{z}_1) \times \prod_{t=2}^T p_{\psi}(\mathbf{y}_t | \mathbf{z}_t) p_{\theta}(\mathbf{z}_t | \mathbf{z}_{t-1})$$

where $\mathbf{z}_t \in \mathbb{R}^L$ are real-valued latent states, θ parameterizes the dynamics and initial condition, and ψ parameterizes the observation model. When the generative model, (θ, ψ) , is known, the statistical inference problem is to compute the smoothing posterior, $p(\mathbf{z}_{1:T} | \mathbf{y}_{1:T})^2$. Otherwise, (θ, ψ) have to be learned from the data – known as system identification⁸.

Variational inference makes it possible to accomplish these goals in a harmonious way. The variational expectation maximization (vEM) algorithm iterates two steps: first, we maximize a lower bound to the log-marginal likelihood – the ELBO – with respect to the parameters of an approximate posterior, $q(\mathbf{z}_{1:T}) \approx p(\mathbf{z}_{1:T} | \mathbf{y}_{1:T})$; then, with the approximate posterior fixed, the ELBO is maximized with respect to parameters of the generative model⁹. For large scale problems, vEM can be slow due to the need to fully optimize the variational parameters before taking gradient steps on parameters of the generative model. Therefore, the variational autoencoder (VAE) is better suited for large scale problems for its ability to simultaneously learn the generative model and inference network – an expressive parametric function that maps data to the parameters of approximate posterior^{10,11}.

Model specifications. Although our approach is applicable to any exponential family state-space process, given their ubiquity, we focus on dynamical systems driven by Gaussian noise so that,

$$p_{\theta}(\mathbf{z}_t | \mathbf{z}_{t-1}) = \mathcal{N}(\mathbf{z}_t | \mathbf{m}_{\theta}(\mathbf{z}_{t-1}), \mathbf{Q}_{\theta}) \quad (1)$$

where $\mathbf{m}_{\theta} : \mathbb{R}^L \rightarrow \mathbb{R}^L$ might be a nonlinear neural network function with learnable parameters θ , and $\mathbf{Q}_{\theta} \in \mathbb{R}^{L \times L}$ is a learnable state-noise covariance matrix. Given the favorable properties of exponential family distributions^{12–15}, especially in the context of variational inference, we write the prior dynamics in their exponential family representation (natural parameter form),

$$p_{\theta}(\mathbf{z}_t | \mathbf{z}_{t-1}) = h(\mathbf{z}_t) \exp(\mathcal{T}(\mathbf{z}_t)^{\top} \boldsymbol{\lambda}_{\theta}(\mathbf{z}_{t-1}) - A(\boldsymbol{\lambda}_{\theta}(\mathbf{z}_{t-1}))) \quad (2)$$

where h is the base measure, $\mathcal{T}(\mathbf{z}_t)$ the sufficient statistics, $A(\cdot)$ the log-partition function, and $\boldsymbol{\lambda}_{\theta}(\cdot)$ is a map $\mathbb{R}^L \mapsto \mathbb{R}^{L^2+L}$ that transforms \mathbf{z}_{t-1} to natural parameters for \mathbf{z}_t . For a Gaussian distribution, the sufficient statistics can be defined as $\mathcal{T}(\mathbf{z}_t)^{\top} = [\mathbf{z}_t^{\top} \quad -\frac{1}{2}\mathbf{z}_t\mathbf{z}_t^{\top}]$, so that $\boldsymbol{\lambda}_{\theta}(\cdot)$ for (1) is given by,

$$\boldsymbol{\lambda}_{\theta}(\mathbf{z}_{t-1}) = \begin{bmatrix} \mathbf{Q}_{\theta}^{-1} \mathbf{m}_{\theta}(\mathbf{z}_{t-1}) \\ \mathbf{Q}_{\theta}^{-1} \end{bmatrix} \quad (\text{dynamics model in natural parameter form}) \quad (3)$$

As it will simplify subsequent analysis, the *mean parameter* mapping corresponding to this natural parameter mapping (guaranteed to exist as long as the exponential family is minimal¹²) is given by

$$\boldsymbol{\mu}_{\theta}(\mathbf{z}_{t-1}) = \mathbb{E}_{p_{\theta}(\mathbf{z}_t | \mathbf{z}_{t-1})}[\mathcal{T}(\mathbf{z}_t)] = \begin{bmatrix} \mathbf{m}_{\theta}(\mathbf{z}_{t-1}) \\ -\frac{1}{2}(\mathbf{m}_{\theta}(\mathbf{z}_{t-1})\mathbf{m}_{\theta}(\mathbf{z}_{t-1})^{\top} + \mathbf{Q}_{\theta}) \end{bmatrix} \quad \begin{pmatrix} \text{mean} \\ \text{parameter} \\ \text{form} \end{pmatrix} \quad (4)$$

Furthermore, we make the following assumptions **i)** the state-noise, \mathbf{Q}_{θ} , is diagonal or structured for efficient matrix-vector multiplications. **ii)** $\mathbf{m}_{\theta}(\cdot)$, is a nonlinear smooth function. **iii)** the likelihood, $p_{\psi}(\mathbf{y}_t | \mathbf{z}_t)$, may be non-conjugate. **iv)** L may be large enough so that L^3 is comparable to T .

Amortized inference for state-space models. A useful property of SSMs is that, \mathbf{z}_t conditioned on \mathbf{z}_{t-1} and $\mathbf{y}_{t:T}$, is independent of $\mathbf{y}_{1:t-1}$, i.e., $p(\mathbf{z}_t | \mathbf{z}_{t-1}, \mathbf{y}_{1:T}) = p(\mathbf{z}_t | \mathbf{z}_{t-1}, \mathbf{y}_{t:T})^{5,16}$. It thus suffices to construct an approximate posterior that factorizes forward in time,

$$q(\mathbf{z}_{1:T}) = q(\mathbf{z}_1) \prod_{t=2}^T q(\mathbf{z}_t | \mathbf{z}_{t-1}) \quad (5)$$

and introduce learnable function approximators to amortize inference by mapping \mathbf{z}_{t-1} and $\mathbf{y}_{t:T}$ to the parameters of $q(\mathbf{z}_t | \mathbf{z}_{t-1})$. This makes it simple to sample $\mathbf{z}_{1:T}$ from the approximate posterior (using the reparameterization trick) and evaluate the ELBO (a.k.a. negative variational free energy),

$$\mathcal{L}(q) = \sum \mathbb{E}_{q_t} [\log p(\mathbf{y}_t | \mathbf{z}_t)] - \mathbb{E}_{q_{t-1}} [\mathbb{D}_{\text{KL}}(q(\mathbf{z}_t | \mathbf{z}_{t-1}) || p_{\theta}(\mathbf{z}_t | \mathbf{z}_{t-1}))] \leq \log p(\mathbf{y}_{1:T}) \quad (6)$$

where $\mathbb{D}_{\text{KL}}(\cdot || \cdot)$ is the Kullback-Leibler (KL) divergence and $\mathbb{E}_{q_t} \equiv \mathbb{E}_{\mathbf{z}_t \sim q(\mathbf{z}_t; \mathbf{y}_{1:T})}$, so that the generative model and inference network parameters can be learned through stochastic backpropagation. Many works for Gaussian $q(\mathbf{z}_t | \mathbf{z}_{t-1})$, such as Krishnan et al.⁶, Alaa and van der Schaar¹⁷, Girin et al.¹⁸, Hafner et al.¹⁹, construct inference networks that parameterize the variational posterior as

$$q(\mathbf{z}_t | \mathbf{z}_{t-1}) = \mathcal{N}(\mathbf{m}_{\phi}(\mathbf{z}_{t-1}, \mathbf{y}_{1:T}), \mathbf{P}_{\phi}(\mathbf{z}_{t-1}, \mathbf{y}_{1:T})). \quad (7)$$

There are limitless ways to construct $\mathbf{m}_{\phi}(\cdot)$ and $\mathbf{P}_{\phi}(\cdot)$ so ϕ can be learned through gradient ascent on the ELBO, but a straightforward and illustrative approach^{6,17} is to transform future data, $\mathbf{y}_{t:T}$, using a recurrent neural network (RNN), or any efficient autoregressive sequence to sequence model, and then mapping the preceding latent state, \mathbf{z}_{t-1} , using a feed-forward neural network, so that a complete inference network description could be,

$$(\mathbf{m}_{\phi}(\mathbf{z}_{t-1}, \mathbf{y}_{t:T}), \mathbf{P}_{\phi}(\mathbf{z}_{t-1}, \mathbf{y}_{t:T})) = \text{NN}([\mathbf{z}_{t-1}, \mathbf{u}_t]), \quad \mathbf{u}_t = \text{S2S}([\mathbf{u}_{t+1}, \mathbf{y}_t]) \quad (8)$$

where S2S(\cdot) is a parametric sequence-to-sequence function that maintains a hidden state \mathbf{u}_t and takes as input \mathbf{y}_t , and NN(\cdot) is a parametric function designed to output approximate posterior parameters. This leads to a backward-forward algorithm, meaning that data $\mathbf{y}_{1:T}$ are mapped to $\mathbf{u}_{1:T}$ in reverse time, and then samples are drawn from $q(\mathbf{z}_t | \mathbf{z}_{t-1})$ forward in time.

Possible drawbacks of this inference framework are **i**) missing observations obstruct inference (the example networks cannot naturally accommodate missing data); **ii**) sampling entire trajectories to approximate the expected KL term can potentially lead to high-variance gradient estimators, and **iii**) statistics of the marginals (e.g. second moments) can only be approximated through sample averages.

3 Related works

Many existing works also consider inference and data driven learning for state-space graphical models through the VAE framework; we highlight the most similar and remark on certain deficits that this work aims to remedy. The structured variational autoencoder (SVAE)²⁰ makes it possible to efficiently evaluate the ELBO while preserving the temporal structure of the posterior by restricting the prior to a *linear dynamical system* (LDS) and then constructing the approximation as $q(\mathbf{z}_{1:T}) \propto p_{\theta}(\mathbf{z}_{1:T}) \prod \exp(t(\mathbf{z}_t)^{\top} \psi(\mathbf{y}_t))$ so that its statistics can be obtained using efficient message passing algorithms. However, the SVAE is not directly applicable when the dynamics are nonlinear since the joint prior will no longer be Gaussian (thereby not allowing for efficient conjugate updates). Recently, Zhao and Linderman²¹ expanded on the SVAE framework by exploiting the LDS structure and associative scan operations to improve its scalability.

The deep Kalman filter (dKF)⁶ uses black-box inference networks to make drawing joint samples from the full posterior simple. However, pure black-box amortization networks such as those can make learning the parameters of the generative model dynamics difficult because their gradients will not propagate through the expected log-likelihood term⁵. In contrast, we consider inference networks inspired by the fundamental importance of the prior for evaluating Bayesian conjugate updates.

The deep variational Bayes filter (dVBF) also considers inference and learning in state-space graphical models⁵. Difficulties of learning the generative model that arise as a result of more standard VAE implementations defining inference networks independent of the prior are handled by forcing samples from the approximate posterior to traverse through the dynamics. Our work extends this concept, by directly specifying the parameters of the variational approximation in terms of the prior.

Our approach constructs an inference network infused with the prior similar to the SVAE and dVBF but i) avoids restrictions to LDS and ii) affords easy access to approximations of the marginal statistics (such as the dense latent state covariances) without having to average over sampled trajectories (or store them directly which would be prohibitive as the latent dimensionality becomes large).

4 Method

Specifying $q(\mathbf{z}_t | \mathbf{z}_{t-1})$. Restricting $q(\mathbf{z}_t | \mathbf{z}_{t-1})$ to be in the same exponential family as the prior dynamics, i.e., Gaussian, requires specifying a mapping from $\mathbf{y}_{t:T}$ and \mathbf{z}_{t-1} to the parameters of a

Gaussian belief for \mathbf{z}_t ; in the example parameterization (8), this was a black-box function returning the parameters in the mean and covariance coordinate-system as $\mathbf{m}_\phi(\mathbf{z}_{t-1}, \mathbf{y}_{t:T})$ and $\mathbf{P}_\phi(\mathbf{z}_{t-1}, \mathbf{y}_{t:T})$. However, since we can readily work in any coordinate-system that might be convenient for analysis, optimization, or computation, it will be favorable to work in the natural parameter coordinates. For that purpose, we express the Gaussian conditional, $q(\mathbf{z}_t | \mathbf{z}_{t-1})$, with a function, $\boldsymbol{\lambda}_\phi(\mathbf{z}_{t-1}, \mathbf{y}_{t:T})$, mapping $\mathbf{y}_{t:T}$ and \mathbf{z}_{t-1} to the natural parameters of \mathbf{z}_t :

$$q(\mathbf{z}_t | \mathbf{z}_{t-1}) \propto \exp(\mathcal{T}(\mathbf{z}_t)^\top \boldsymbol{\lambda}_\phi(\mathbf{z}_{t-1}, \mathbf{y}_{t:T})) \quad (9)$$

Enforcing minimality makes it so that if $\boldsymbol{\lambda}_\phi(\cdot)$ is expressive enough, then the parameterization of (8) could be recovered for some setting of the inference network parameters ϕ . The natural parameters are the precision-scaled mean, $\mathbf{h}_\phi(\mathbf{z}_{t-1}, \mathbf{y}_{t:T})$, and the precision, $\mathbf{J}_\phi(\mathbf{z}_{t-1}, \mathbf{y}_{t:T})$, which can be written in the mean-covariance coordinate system as

$$\boldsymbol{\lambda}_\phi(\mathbf{z}_{t-1}, \mathbf{y}_{t:T}) = \begin{bmatrix} \mathbf{h}_\phi(\mathbf{z}_{t-1}, \mathbf{y}_{t:T}) \\ \mathbf{J}_\phi(\mathbf{z}_{t-1}, \mathbf{y}_{t:T}) \end{bmatrix} = \begin{bmatrix} \mathbf{P}_\phi^{-1}(\mathbf{z}_{t-1}, \mathbf{y}_{t:T}) \mathbf{m}_\phi(\mathbf{z}_{t-1}, \mathbf{y}_{t:T}) \\ \mathbf{P}_\phi^{-1}(\mathbf{z}_{t-1}, \mathbf{y}_{t:T}) \end{bmatrix} \quad (10)$$

Instead of a black-box parameterization for $\boldsymbol{\lambda}_\phi(\cdot, \cdot)$, we draw inspiration from a quintessential facet of conjugate Bayesian inference: natural parameters of the posterior are a sum-separable combination of the natural parameters of the prior in addition to a data dependent term^{12,22}. This suggests an appealing decomposition of the conditional variational posterior natural parameter mapping as,

$$\boldsymbol{\lambda}_\phi(\mathbf{z}_{t-1}, \mathbf{y}_{t:T}) = \boldsymbol{\lambda}_\theta(\mathbf{z}_{t-1}) + \tilde{\boldsymbol{\lambda}}_\phi(\mathbf{y}_{t:T}) \quad (11)$$

where $\boldsymbol{\lambda}_\theta(\mathbf{z}_{t-1})$, intrinsic in the specification of $p_\theta(\mathbf{z}_t | \mathbf{z}_{t-1})$, maps \mathbf{z}_{t-1} to the space of natural parameters for \mathbf{z}_t according to (3). The term, $\tilde{\boldsymbol{\lambda}}_\phi(\mathbf{y}_{t:T}) := \tilde{\boldsymbol{\lambda}}_t$, can now be thought of as a data dependent update to the prior for a conjugate *pseudo-observation*, $\tilde{\mathbf{y}}_t$, with likelihood

$$p(\tilde{\mathbf{y}}_t | \mathbf{z}_t) \propto \exp(\mathcal{T}(\mathbf{z}_t)^\top \tilde{\boldsymbol{\lambda}}_t) \quad (12)$$

Importantly, pseudo-observations defined this way encode the current *and* future observations of the raw data – an essential component for transforming the statistical smoothing problem into an alternative filtering problem. When the pseudo-observation likelihood is defined by (12), the conditional variational posterior can be rewritten as

$$q(\mathbf{z}_t | \mathbf{z}_{t-1}) \propto \exp(\mathcal{T}(\mathbf{z}_t)^\top (\tilde{\boldsymbol{\lambda}}_t + \boldsymbol{\lambda}_\theta(\mathbf{z}_{t-1}))) = p(\tilde{\mathbf{y}}_t | \mathbf{z}_t) p_\theta(\mathbf{z}_t | \mathbf{z}_{t-1}) \quad (13)$$

This allows us to write the joint variational approximation given by (5) compactly as,

$$q(\mathbf{z}_{1:T}) = \prod p(\tilde{\mathbf{y}}_t | \mathbf{z}_t) p_\theta(\mathbf{z}_{1:T}) / p(\tilde{\mathbf{y}}_{1:T}) \quad (14)$$

Forcing the posterior computation to be amortized using the prior dynamics introduces an inductive bias that ties the performance of the inference network to the quality of the generative model.

Approximate posterior inference (smoothing) as filtering. Substituting (14) into (94) gives,

$$\mathcal{L}(q) = \sum \mathbb{E}_{q_t} [\log p(\mathbf{y}_t | \mathbf{z}_t)] - \mathbb{E}_{q_t} [\log p(\tilde{\mathbf{y}}_t | \mathbf{z}_t)] + \log p(\tilde{\mathbf{y}}_{1:T}) \quad (15)$$

The dependence on θ is now implicit in the log marginal likelihood of the pseudo-observations. This resembles the ELBO derived in Hamelijncx et al.²³ for state-space Gaussian Processes with two caveats: **i**) in our case, nonlinearity of the dynamics make $p(\tilde{\mathbf{y}}_{1:T})$ intractable, and **ii**) expectations with respect to the non-Gaussian marginals, q_t , are intractable. As an alternative to a sampling based solution, we introduce another probability measure that approximates the marginals as Gaussian distributions, i.e., $\pi(\mathbf{z}_t) \approx q(\mathbf{z}_t; \mathbf{y}_{1:T})$ such that the modified ELBO approximates (15):

$$\mathcal{L}(q) \approx \sum \mathbb{E}_{\pi_t} [\log p(\mathbf{y}_t | \mathbf{z}_t)] - \mathbb{E}_{\pi_t} [\log p(\tilde{\mathbf{y}}_t | \mathbf{z}_t)] + \log p(\tilde{\mathbf{y}}_{1:T}) \quad (16)$$

Our idea is to parameterize the approximate marginal distributions, $\pi(\mathbf{z}_t)$, in a way that makes approximating $\log p(\tilde{\mathbf{y}}_{1:T})$ convenient. The first step in proceeding forward is to note that since a single pseudo-observation $\tilde{\mathbf{y}}_t$ encodes information of $\mathbf{y}_{t:T}$, the filtering distribution given the pseudo-observations should be able to approximate the smoothing distribution for the raw data, i.e.,

$$p(\mathbf{z}_t | \tilde{\mathbf{y}}_{1:t}) \approx p(\mathbf{z}_t | \mathbf{y}_{1:T}). \quad (17)$$

Consequently, if $\pi(\mathbf{z}_t)$ are constructed as approximate filtering distributions given pseudo-observations, so that $\pi(\mathbf{z}_t) \approx p(\mathbf{z}_t | \tilde{\mathbf{y}}_{1:t})$, then not only do they approximate the posterior marginal, they also make approximating $p(\tilde{\mathbf{y}}_{1:T})$ straightforward. Since $p(\tilde{\mathbf{y}}_t | \mathbf{z}_t)$ are Gaussian potentials, if $\pi(\mathbf{z}_t)$ is a Gaussian approximation to the filtering distribution of the pseudo-observations, so that $\pi(\mathbf{z}_t) \approx p(\mathbf{z}_t | \tilde{\mathbf{y}}_{1:t}) \propto p(\tilde{\mathbf{y}}_t | \mathbf{z}_t) p(\mathbf{z}_t | \tilde{\mathbf{y}}_{1:t-1})$, then it is natural to factorize $\pi(\mathbf{z}_t)$ similarly so that,

$$\pi(\mathbf{z}_t) \propto p(\tilde{\mathbf{y}}_t | \mathbf{z}_t) \bar{\pi}(\mathbf{z}_t) \quad (18)$$

where $\bar{\pi}(\mathbf{z}_t)$ is a Gaussian approximation to the one-step filtering predictive distribution given the pseudo-observations (to be specified in (27)),

$$\bar{\pi}(\mathbf{z}_t) \approx \bar{p}(\mathbf{z}_t | \tilde{\mathbf{y}}_{1:t-1}) = \mathbb{E}_{p(\mathbf{z}_{t-1} | \tilde{\mathbf{y}}_{1:t-1})} [p_{\theta}(\mathbf{z}_t | \mathbf{z}_{t-1})] \quad (19)$$

Exploiting the graphical model structure in order to make the approximation,

$$\log p(\tilde{\mathbf{y}}_{1:T}) = \sum_t \log \left[\int p(\tilde{\mathbf{y}}_t | \mathbf{z}_t) p(\mathbf{z}_t | \tilde{\mathbf{y}}_{1:t-1}) d\mathbf{z}_t \right] \approx \sum_t \log \mathbb{E}_{\bar{\pi}_t} [p(\tilde{\mathbf{y}}_t | \mathbf{z}_t)] \quad (20)$$

leads to an alternative approximation to the ELBO, which itself is an ELBO,

Variational smoothing ELBO

$$\hat{\mathcal{L}}(\pi) = \sum \mathbb{E}_{\pi_t} [\log p(\mathbf{y}_t | \mathbf{z}_t)] - \mathbb{E}_{\pi_t} [\log p(\tilde{\mathbf{y}}_t | \mathbf{z}_t)] + \log \mathbb{E}_{\bar{\pi}_t} [p(\tilde{\mathbf{y}}_t | \mathbf{z}_t)] \quad (21)$$

$$= \sum \mathbb{E}_{\pi_t} [\log p(\mathbf{y}_t | \mathbf{z}_t)] - \mathbb{D}_{\text{KL}}(\pi(\mathbf{z}_t) || \bar{\pi}(\mathbf{z}_t)) \quad (22)$$

Written this way, it is clear that as a learning objective, (22) encourages models where the posterior at time t remains close to the one-step posterior predictive at time t (which depends on the generative model and the posterior at time $t - 1$). Before discussing a procedure for finding approximations to the filtering distribution given pseudo-observations, we describe how to efficiently design the Gaussian inference network producing the pseudo-observation parameters.

Local and backward encoders. In a state-space graphical model, the latent state posterior should be accessible for every time point even with missing observations. To enable the amortized inference network to process missing observations in a principled way, we decompose the natural parameter update into two additive components: **i**) a *local* encoder, $\alpha_{\phi}(\cdot)$, for current observation, and **ii**) a *backward* encoder, $\beta_{\phi}(\cdot)$, for future observations, i.e.,

$$\tilde{\lambda}_{\phi}(\mathbf{y}_{t:T}) = \alpha_{\phi}(\mathbf{y}_t) + \beta_{\phi}(\mathbf{y}_{t+1:T}) \quad (\text{or for the sake of brevity}) \quad \tilde{\lambda}_t = \alpha_t + \beta_{t+1} \quad (23)$$

Furthermore, by building the dependence of $\beta_{\phi}(\cdot)$ on $\mathbf{y}_{t+1:T}$ through their representation as $\alpha_{t+1:T}$, so that $\beta_{\phi}(\mathbf{y}_{t+1:T}) = \beta_{\phi}(\alpha_{t+1:T})$, a missing observation at time t is handled by setting $\alpha_t = \mathbf{0}$. While a data dependent natural parameter update of $\mathbf{0}$ faithfully represents a missing observation – in the absence of data, the prior should not be updated – alternatively setting $\mathbf{y}_t = \mathbf{0}$ would introduce a harmful inductive bias into the inference network, since an observation of $\mathbf{0}$ can be arbitrarily informative. Given the impracticality of $\mathcal{O}(TL^2)$ memory requirements, it is appealing to consider a low-rank parameterization for the local and backward encoders – we consider

$$\alpha_t = \begin{pmatrix} \mathbf{a}_t \\ \mathbf{A}_t \mathbf{A}_t^{\top} \end{pmatrix} := \begin{pmatrix} \mathbf{a}(\mathbf{y}_t) \\ \mathbf{A}(\mathbf{y}_t) \mathbf{A}(\mathbf{y}_t)^{\top} \end{pmatrix} \quad \beta_t = \begin{pmatrix} \mathbf{b}_t \\ \mathbf{B}_t \mathbf{B}_t^{\top} \end{pmatrix} := \begin{pmatrix} \mathbf{b}(\alpha_{t:T}) \\ \mathbf{B}(\alpha_{t:T}) \mathbf{B}(\alpha_{t:T})^{\top} \end{pmatrix} \quad (24)$$

where $\mathbf{A}_t \in \mathbb{R}^{L \times r_{\alpha}}$ with $\mathbf{B}_t \in \mathbb{R}^{L \times r_{\beta}}$ parameterize low-rank local/backward precision updates, and $\mathbf{a}_t \in \mathbb{R}^L$ with $\mathbf{b}_t \in \mathbb{R}^L$ parameterize local/backward precision-scaled mean updates. Using these descriptions and the additive decomposition (23), the parameters of a single pseudo observation are,

$$\tilde{\lambda}_t = \begin{pmatrix} \mathbf{k}_t \\ \mathbf{K}_t \mathbf{K}_t^{\top} \end{pmatrix} := \begin{pmatrix} \mathbf{k}(\mathbf{y}_{t:T}) \\ \mathbf{K}(\mathbf{y}_{t:T}) \mathbf{K}(\mathbf{y}_{t:T})^{\top} \end{pmatrix} = \begin{pmatrix} \mathbf{a}_t + \mathbf{b}_t \\ [\mathbf{A}_t \ \mathbf{B}_t] [\mathbf{A}_t \ \mathbf{B}_t]^{\top} \end{pmatrix} \quad (25)$$

where $\mathbf{K} \in \mathbb{R}^{L \times r}$ if $r = r_{\alpha} + r_{\beta}$ and $\mathbf{k} \in \mathbb{R}^L$. The low-rank structure of the natural parameter updates will be a key component to develop an efficient approximate message passing algorithm for obtaining sufficient statistics of the approximate posterior and evaluating the ELBO. Analogous to the inference network description (8), a differentiable architecture producing $\alpha_{1:T}$ and $\beta_{1:T}$ could be,

$$\alpha_t = \text{NN}(\mathbf{y}_t) \quad \beta_t = \text{S2S}([\beta_{t+1}, \alpha_t]), \quad (26)$$

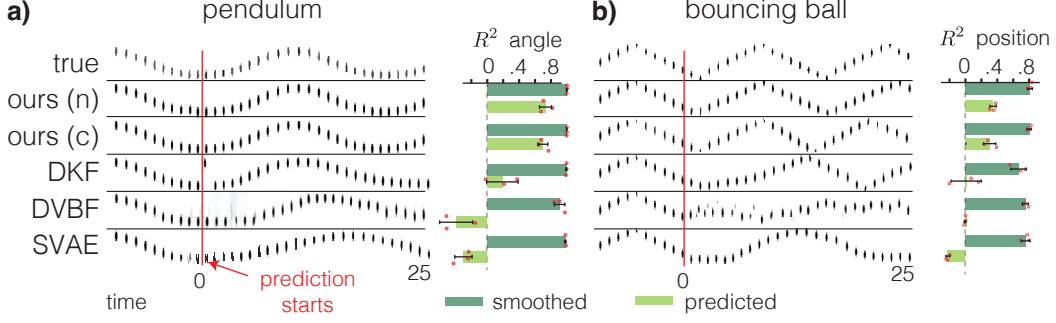


Figure 1: **Smoothing and predictive performance on bouncing ball and pendulum.** To the left of the red line are samples from the posterior during the data window projected to image space, to the right of the red line are samples unrolled from $p_{\theta}(\mathbf{z}_t | \mathbf{z}_{t-1})$. **a)** while all methods are adept at smoothing in the context window, our methods predictive performance is better by a noticeable margin as measured by the R^2 . **b)** similar results hold for the bouncing ball dataset.

which overall defines the map $\mathbf{y}_{1:T} \mapsto (\boldsymbol{\alpha}_{1:T}, \boldsymbol{\beta}_{1:T})$. An added benefit of separating local and backward encoders is potential reduction in parameter count for the backward encoder when $L < N$.

Differentiable nonlinear filtering. How can we obtain differentiable approximations to the filtering distribution under the pseudo-observations? A straightforward approach is to take a single forward pass through the pseudo-observations and produce a series of approximate filtering and predictive distributions by propagating approximate messages recursively as follows:

$$(i) \quad \bar{\pi}(\mathbf{z}_t) = \operatorname{argmin} \mathbb{D}_{\text{KL}}(\mathbb{E}_{\pi_{t-1}} [p_{\theta}(\mathbf{z}_t | \mathbf{z}_{t-1})] || \bar{\pi}(\mathbf{z}_t)) \implies \bar{\boldsymbol{\mu}}_t = \mathbb{E}_{\pi_{t-1}} [\boldsymbol{\mu}_{\theta}(\mathbf{z}_{t-1})] \quad (27)$$

$$(ii) \quad \pi(\mathbf{z}_t) = \operatorname{argmin} \mathbb{D}_{\text{KL}}(\pi(\mathbf{z}_t) || p(\tilde{\mathbf{y}}_t | \mathbf{z}_t) \bar{\pi}(\mathbf{z}_t)) \implies \boldsymbol{\lambda}_t = \bar{\boldsymbol{\lambda}}_t + \tilde{\boldsymbol{\lambda}}_t \quad (28)$$

In case of linear dynamics, the parameters of $\bar{\pi}(\mathbf{z}_t)$ minimizing (27) can be found exactly; otherwise, Monte Carlo integration can provide a differentiable approximation. However, the conjugacy structure of the inference networks guarantee the solution of (28) is exact.

Exploiting sample approximation structure. In the case of variational Gaussian approximations, if Monte-Carlo integration is used to find a differentiable approximation of the mean parameters of $\bar{\pi}(\mathbf{z}_t)$ that minimize (27) by setting $\bar{\boldsymbol{\mu}}_t = 1/S \sum_s \boldsymbol{\mu}_{\theta}(\mathbf{z}_{t-1}^s)$ for $\mathbf{z}_{t-1}^s \sim \pi(\mathbf{z}_{t-1})$ then, the sample approximation of the mean and covariance become

$$\bar{\mathbf{m}}_t = 1/S \sum_{s=1}^S \mathbf{m}_{\theta}(\mathbf{z}_{t-1}^s) \quad \bar{\mathbf{P}}_t = \bar{\mathbf{M}}_t^c \bar{\mathbf{M}}_t^{c\top} + \mathbf{Q}_{\theta} \quad (29)$$

where S is the sample size, and $\bar{\mathbf{M}}_t^c = 1/\sqrt{S} [\mathbf{m}_{\theta}(\mathbf{z}_{t-1}^1) - \bar{\mathbf{m}}_t, \dots, \mathbf{m}_{\theta}(\mathbf{z}_{t-1}^S) - \bar{\mathbf{m}}_t] \in \mathbb{R}^{L \times S}$ is the matrix of centered samples passed through the dynamics. Importantly, Eq. (29) indicates that $\bar{\mathbf{P}}_t$ will have a low-rank plus diagonal structure if $S < L$, which allows for efficient matrix-vector multiplications (MVM). Evaluating $\bar{\mathbf{h}}_t = \bar{\mathbf{P}}_t^{-1} \bar{\mathbf{m}}_t$ and MVMs with $\bar{\mathbf{P}}_t^{-1}$, can be carried out in $\mathcal{O}(LS + S^2)$ time, after an initial cost of $\mathcal{O}(LS^2 + S^3)$ to factorize $\tilde{\boldsymbol{\Upsilon}}_t \tilde{\boldsymbol{\Upsilon}}_t^{\top} = (\mathbf{I}_S + \bar{\mathbf{M}}_t^{c\top} \mathbf{Q}_{\theta}^{-1} \bar{\mathbf{M}}_t^c)^{-1}$, by applying the Woodbury identity to (29),

$$\bar{\mathbf{P}}_t^{-1} = \mathbf{Q}_{\theta}^{-1} - \mathbf{Q}_{\theta}^{-1} \bar{\mathbf{M}}_t^c \tilde{\boldsymbol{\Upsilon}}_t \tilde{\boldsymbol{\Upsilon}}_t^{\top} \bar{\mathbf{M}}_t^{c\top} \mathbf{Q}_{\theta}^{-1} \quad (30)$$

Since this specifies all quantities that characterize $\bar{\pi}(\mathbf{z}_t)$, following (28), next is to update our belief by adding the information from the pseudo observation to them,

$$\mathbf{h}_t = \bar{\mathbf{h}}_t + \mathbf{k}_t \quad \mathbf{P}_t^{-1} = \bar{\mathbf{P}}_t^{-1} + \mathbf{K}_t \mathbf{K}_t^{\top} \quad (31)$$

As a result, the multiplication in $\mathbf{m}_t = \mathbf{P}_t \mathbf{h}_t$ requires $\mathcal{O}(LS + Lr)$ time, and, analogous to (30), the square root factor $\boldsymbol{\Upsilon}_t$ in

$$\mathbf{P}_t = \bar{\mathbf{P}}_t - \bar{\mathbf{P}}_t \mathbf{K}_t \boldsymbol{\Upsilon}_t \boldsymbol{\Upsilon}_t^{\top} \mathbf{K}_t^{\top} \bar{\mathbf{P}}_t \quad (32)$$

requires $\mathcal{O}(r^3 + LSr + S^2r)$ time where $\boldsymbol{\Upsilon}_t \boldsymbol{\Upsilon}_t^{\top} = (\mathbf{I}_r + \mathbf{K}_t^{\top} \bar{\mathbf{P}}_t \mathbf{K}_t)^{-1}$. In the case of a linear

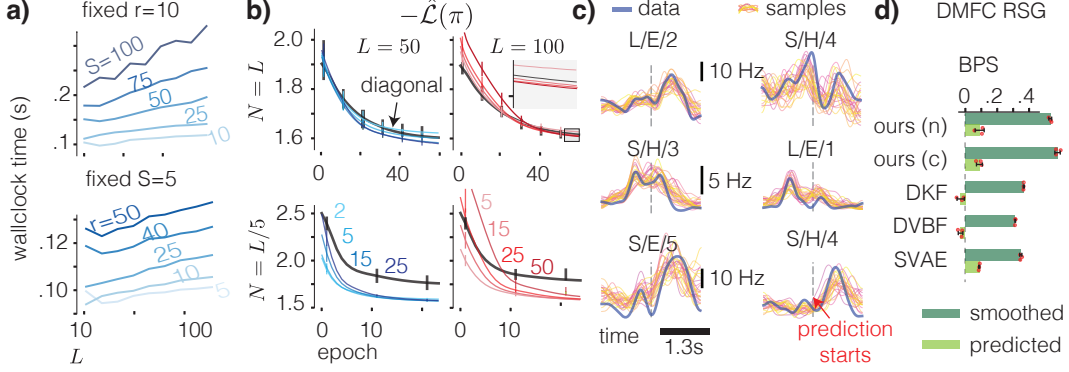


Figure 2: **a)** Empirical time complexity scaling. Since complexity is a function of L , S , and r , we vary L (top) for fixed S and (bottom) for fixed r ; we examine several values of the variable not fixed. Recording the wall-clock time shows that our implementation scales linearly in L . **b)** (top) Negative ELBO as a function of training epoch when $N = L$ (bottom) when $N = L/5$; the left column shows the case $L = 50$ and the right when $L = 100$. Different colors indicate different settings of the local/backward encoder rank; zooming in for $L = 100$, shows low-rank updates can match diagonal ones. **c)** Peristimulus time histogram (PSTH) for the DMFC RSG dataset; we use a context window of 1.3s and a prediction window of 1.3s. **d)** BPS for each method for context/prediction windows.

and Gaussian SSM, iterating (27) and (28) recover the exact Kalman filtering algorithm, and in the non-conjugate it can be considered an approximate sum-product algorithm. The end result is an approximate filtering algorithm, where in the case that L is significantly larger than S or r , has complexity of $\mathcal{O}(L(Sr + r^2 + S^2))$ per step, made possible by **1)** the structured covariance produced by the Monte Carlo moment matching approximations **2)** the low rank structure of the filtering precision resulting from specification of the inference networks **3)** neither \mathbf{P}_t , \mathbf{P}_t , or their inverses need to be explicitly constructed.

Efficient sampling and ELBO evaluations. When $\mathbb{E}_{\pi_t} [\log p(\mathbf{y}_t | \mathbf{z}_t)]$ can not be evaluated in closed form, Monte-Carlo integration can be used as a differentiable approximation. To sample from $\pi(\mathbf{z}_t)$ without explicitly constructing \mathbf{P}_t , we can take $\bar{\mathbf{z}}_t^s \sim \mathcal{N}(\mathbf{0}, \bar{\mathbf{P}}_t)$ and $\mathbf{w}_t^s \sim \mathcal{N}(\mathbf{0}, \mathbf{I}_{L+S})$ and set,

$$\mathbf{z}_t^s = \mathbf{m}_t + \bar{\mathbf{z}}_t^s - \mathbf{K}_t \Upsilon_t \Upsilon_t^\top (\mathbf{K}_t^\top \bar{\mathbf{z}}_t^s + \mathbf{w}_t^s). \quad (33)$$

While more details are provided in App. B.3, this can be done efficiently since samples can be drawn cheaply from $\bar{\pi}(\mathbf{z}_t)$ using Eq. (29). Whereas Monte-Carlo approximations of the expected log-likelihood term might be unavoidable, the closed form solution for the KL between two Gaussian distributions should be used to avoid further stochastic approximations. The only difficulty, is that the time complexity of naively evaluating the KL term,

$$\mathbb{D}_{\text{KL}}(\pi(\mathbf{z}_t) || \bar{\pi}(\mathbf{z}_t)) = \frac{1}{2} [(\bar{\mathbf{m}}_t - \mathbf{m}_t)^\top \bar{\mathbf{P}}_t^{-1} (\bar{\mathbf{m}}_t - \mathbf{m}_t) + \text{tr}(\bar{\mathbf{P}}_t^{-1} \mathbf{P}_t) + \log(|\bar{\mathbf{P}}_t|/|\mathbf{P}_t|) - L] \quad (34)$$

scales $\mathcal{O}(L^3)$. However, since matrix vector multiplies with $\bar{\mathbf{P}}_t^{-1}$ can be performed efficiently and the trace/log-determinant terms can be rewritten using the square-root factors acquired during the forward pass, as we describe in App. C.1, it is possible to evaluate the KL in $\mathcal{O}(LSr + LS^2 + Lr^2)$ time. After a complete forward pass through the encoded data, we acquire the samples $\mathbf{z}_{1:T}^{1:S}$ and all necessary quantities for efficient ELBO evaluation. We detail the variational filtering algorithm in Alg. 2 in App. C.2 and the complete end-to-end learning procedure in Alg. 1.

Causal amortized inference for streaming data. In constructing a fully differentiable variational approximation, the parameters of the approximate marginals were effectively amortized according to a recursion in the natural parameter space by iterating Eqs. (27) and (28). This recursion can be recognized more easily by introducing the function, $\tilde{\mathfrak{F}}_\theta(\cdot)$, and writing

$$\lambda_t = \tilde{\mathfrak{F}}_\theta(\lambda_{t-1}) + \alpha_t + \beta_{t+1} \quad \text{where} \quad \tilde{\mathfrak{F}}_\theta(\lambda_{t-1}) = \nabla A^* \left(\int \pi(\mathbf{z}_{t-1}; \lambda_{t-1}) \mu_\theta(\mathbf{z}_{t-1}) \right), \quad (35)$$

$\nabla A^* : (\mathbf{m}, -\frac{1}{2}(\mathbf{P} + \mathbf{m}\mathbf{m}^\top)) \mapsto (\mathbf{P}^{-1}\mathbf{m}, \mathbf{P}^{-1})$, and $A^*(\cdot)$ is the convex conjugate of the log-partition function¹². So that, $\tilde{\mathfrak{F}}_\theta(\cdot)$ can be thought of as mapping λ_{t-1} forward in time by first

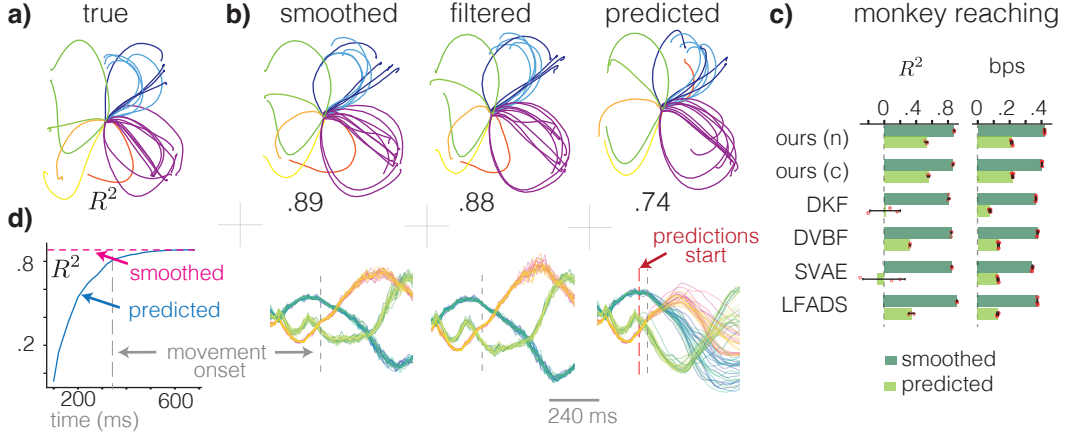


Figure 3: **Predict behavior from a causally inferred initial condition.** **a)** Actual reaches. **b)** (top) Reaches linearly decoded from smoothed ($R^2 = 0.89$), causally filtered ($R^2 = 0.88$), & predicted ($R^2 = 0.74$) latent trajectories starting from an initial condition causally inferred during the preparatory period. (bottom) Top 3 principal latent dimensions per regime (smoothing/filtering/prediction) for three example trials. **c)** bps / R^2 of predicted hand velocity using rates inferred from the 700ms context window and the 500ms prediction window. **d)** Velocity decoding R^2 using predicted trajectories as a function of how far into the trial the latent state was filtered until it was only sampled from the autonomous dynamics; by the the movement onset, behavioral predictions using latent trajectory predictions are nearly on par with behavior decoded from the smoothed posterior.

taking the expectation of (4) with respect to $\pi(\mathbf{z}_{t-1}; \lambda_{t-1})$, and then applying the mean-to-natural coordinate transformation.

One deficiency of amortizing inference through recursion (35) is the inability to produce approximations to the filtering distributions, $p(\mathbf{z}_t | \mathbf{y}_{1:t})$, which may be useful in streaming/online settings or for testing hypothesis of causality. However, since (22) is impartial to how the variational parameters are constructed, an alternative sequence-to-sequence map for λ_t could be defined by,

$$\lambda_t = \underbrace{\mathfrak{F}_\theta(\lambda_{t-1} - \beta_t)}_{\text{smoothed-future}} + \alpha_t + \beta_{t+1}, \quad (36)$$

so that $\check{\lambda}_t$ ($\check{\lambda}_t \equiv \lambda_t - \beta_{t+1}$) obey the recursion $\check{\lambda}_t = \mathfrak{F}_\theta(\check{\lambda}_{t-1}) + \alpha_t$ and are natural parameters of an approximate filtering distribution, $\tilde{\pi}(\mathbf{z}_t) \approx p(\mathbf{z}_t | \mathbf{y}_{1:t})$. Consequently the approximations to posterior and predictive distributions will have a more complicated relationship than they previously did; while efficient sampling and ELBO evaluation are more intricate as a result – linear time scaling in the state-dimension can still be achieved with additional algebraic manipulations, as we show in App. C.2.

5 Experiments

Time complexity & low-rank precision updates. To motivate dense variational Gaussian approximations – particularly for state-space graphical models – consider that interactions between latent states occur through $p_\theta(\mathbf{z}_t | \mathbf{z}_{t-1})$ and $p_\psi(\mathbf{y}_t | \mathbf{z}_t)$. While Gaussian approximations with dense and full-rank covariance should outperform a diagonal covariance alternative, we wondered whether low-rank approximations could outperform their diagonal counterparts for high-dimensional dynamical systems. We simulated data from 50D and 100D linear dynamical systems and compared the convergence between dense and diagonal approximations (Fig. 2b); we examined the ELBO for

Algorithm 1 End-to-end learning

Input: $\mathbf{y}_{1:T}$
while not converged **do**
 for $t = T$ **to** 1 **do**
 $\alpha_t = \text{NN}(\mathbf{y}_t)$ # local encoder
 $\beta_t = \text{S2S}([\beta_{t+1} \ \alpha_t])$ # backward encoder
 $\mathbf{k}_t = \mathbf{a}_t + \mathbf{b}_t$
 $\mathbf{K}_t = [\mathbf{A}_t \ \mathbf{B}_t]$
 end for
 $\mathbf{z}_{1:T}^S, \mathbf{m}_{1:T}, \bar{\mathbf{m}}_{1:T}, \Upsilon_{1:T} = \text{Alg. 2}(\mathbf{k}_{1:T}, \mathbf{K}_{1:T})$
 $\hat{\mathcal{L}}(\pi) = \sum [S^{-1} \sum \log p(\mathbf{y}_t | \mathbf{z}_t^s) - \mathbb{D}_{\text{KL}}(\pi_t || \bar{\pi}_t)]$
 $(\phi, \theta, \psi) \leftarrow (\phi, \theta, \psi) - \nabla \hat{\mathcal{L}}(\pi)$
end while
Output: $\mathbf{z}_{1:T}^S, \mathbf{m}_{1:T}, \bar{\mathbf{m}}_{1:T}, \Upsilon_{1:T}$

different rank parameterizations in two regimes **i**) observations and states are of the same dimensionality, $N = L$, and **ii**) observations are lower dimensional than states, $N = L/5$. While not surprising that dense variational Gaussian approximations can achieve superior performance, message passing in latent Gaussian models with dense covariance costs $\mathcal{O}(L^3)$ ²⁴. In Fig. 2a, we demonstrate that our inference algorithm is able to achieve $\mathcal{O}(L)$ time complexity using structured covariances – making dense approximations more amenable to higher-dimensional dynamical systems.

Baseline comparisons – pendulum & bouncing ball. Next, we validated the efficacy of our approach in learning complex dynamical systems through high-dimensional nonlinear observations by considering **i**) a pendulum system²⁵ and **ii**) a bouncing ball^{26,27}. An interesting aspect of these datasets is that images can be reconstructed with impartial knowledge of the latent state, but for accurate long-term predictions, the dynamics will need to propagate features of the latent state that are irrelevant to the likelihood (e.g. pendulum angular velocity). For benchmarks, three other deep SSM approaches were included: **i**) deep variational Bayes filter(DVBF)⁵ **ii**) deep Kalman filter(DKF)²⁸ **iii**) structured VAE(SVAE)²⁰. We denote our causal amortization network with (c) and the noncausal version with (n). We trained all models in context windows of 50 consecutive images and then sampled future 50 / 25 time-step latent states from the learned dynamical system for pendulum / bouncing ball. To measure quality of learned latent representation and dynamics, we fitted angular velocity / position decoders from training set latent states, and then tested them on the held-out context (smoothing) and forecast (prediction) windows. Fig. 1 shows that, while all methods are able to reconstruct well in context windows, our method exhibits more predictive power.

Neural population dynamics. We consider two neuroscientific datasets where previous studies have shown the importance of population dynamics in generating plausible hypothesis about underlying neural computation. In addition DKF, DVBF, and SVAE, we added the LFADS method⁷. First, we considered the motor cortex recording of a monkey performing a reaching task²⁹ and evaluate the methods’ ability of forecasting neural spiking and behavioral correlates. We measure the performance by bits-per-spike (BPS) using inferred spike-train rates³⁰ and R^2 for decoding hand velocity. Similar to the previous experiment, we evaluate the performance in two regimes: **i**) a 700ms context window and **ii**) a 500ms prediction window following an initial context window of 200ms. Fig. 3c shows again that, while all the methods excel at smoothing in the context window, our method makes more informative predictions in terms of R^2 and BPS. Next, we examined a causally amortized inference network in more depth by considering how well the monkey’s behavior can be decoded in three regimes: smoothing, filtering, and prediction. Fig. 3b shows that hand velocity can be decoded nearly as well in the filtering regime (without access to future data) as in the smoothing regime; furthermore, prediction starting prior to movement onset exhibits remarkable quality.

Secondly, we examined neural recordings of a monkey performing timing interval reproduction task³¹. During this task, the monkey observes a random interval of time (termed the ‘ready’-‘set’ period) demarcated by two cues, and the goal of the monkey is to reproduce that interval (termed the ‘set’-‘go’ period). We perform a similar procedure as before, but for this experiment we use the period before ‘set’ as the context window, and use the learned dynamics to make predictions onward; in Fig. 2d we show our performance metrics and example sample PSTH’s from the learned model.

6 Discussion

Neural computation is inherently nonlinear; hence, system identification methods that allow nonlinear dynamical system modeling are crucial for advancing neuroscience. General SSMs can perform well on inferring smoothed latent state trajectories *without* learning a good model of the nonlinear dynamics. Our proposed method, XFADS, can not only perform efficient system identification and smoothing but also forecast future state evolution for population recordings—a hallmark of a meaningful nonlinear dynamical model; using a causal inference network, XFADS can be used for real-time monitoring, feedback control, and online optimal experimental design, opening the door for new kinds of basic and clinical neuroscience experiments. Future work will focus on developing network architectures for precision matrix updates that are more parameter efficient when the rank those updates become moderate. Furthermore, depending on generative model specifications, such as L , while the inference framework of Alg. 1 is always applicable, modifications of the message passing procedure in Alg. 2 might be necessary to maximize efficiency (e.g. if L is small but S is large); maximally efficient inference algorithms should also be able to adaptively schedule the number of samples for Monte-Carlo approximations during training.

References

- [1] Kailath, T., Sayed, A. H. & Hassibi, B. *Linear estimation*. Prentice Hall, 2000.
- [2] Särkkä, S. *Bayesian filtering and smoothing*. Cambridge University Press, 2013. ISBN 9781107619289.
- [3] Anderson, B. D. O. & Moore, J. B. *Optimal Filtering*. Prentice-Hall, Englewood Cliffs, N.J., 1979. ISBN 978-0-13-638122-8.
- [4] Kingma, D. P. & Welling, M. Auto-Encoding variational bayes. In *International Conference on Learning Representation*, May 2014.
- [5] Karl, M., Soelch, M., Bayer, J. & Smagt, P.van der . Deep variational Bayes filters: Unsupervised learning of state space models from raw data. In *International Conference on Learning Representations*, 2017.
- [6] Krishnan, R. G., Shalit, U. & Sontag, D. A. Structured inference networks for nonlinear state space models. In *AAAI Conference on Artificial Intelligence*, 2016.
- [7] Pandarinath, C., O’Shea, D. J., Collins, J., Jozefowicz, R., Stavisky, S. D., Kao, J. C., Trautmann, E. M., Kaufman, M. T., Ryu, S. I., Hochberg, L. R. & others, . Inferring single-trial neural population dynamics using sequential auto-encoders. *Nature methods*, 15(10):805–815, 2018.
- [8] Van Overschee, P. & De Moor, B. *Subspace identification for linear systems*. Springer US, Boston, MA, 1996. ISBN 9781461380610,9781461304654.
- [9] Turner, R. E. & Sahani, M. Two problems with variational expectation maximisation for time-series models. In Barber, D., Cemgil, T. & Chiappa, S., editors, *Bayesian Time series models*, chapter 5, pages 109–130. Cambridge University Press, 2011.
- [10] Kingma, D. P. & Ba, J. Adam: A method for stochastic optimization. *arXiv preprint arXiv:1412.6980*, 2014.
- [11] Rezende, D. J., Mohamed, S. & Wierstra, D. Stochastic backpropagation and approximate inference in deep generative models. In *International conference on machine learning*, pages 1278–1286. PMLR, 2014.
- [12] Wainwright, M. J. & Jordan, M. I. Graphical models, exponential families, and variational inference. *Foundations and Trends in Machine Learning*, 1(1–2):1–305, 2008.
- [13] Diaconis, P. & Ylvisaker, D. Conjugate priors for exponential families. *The Annals of statistics*, pages 269–281, 1979.
- [14] Seeger, M. Expectation propagation for exponential families. Technical report, University of California at Berkeley, 2005.
- [15] Khan, M. & Lin, W. Conjugate-Computation Variational Inference : Converting Variational Inference in Non-Conjugate Models to Inferences in Conjugate Models. In Singh, A. & Zhu, J., editors, *Proceedings of the 20th International Conference on Artificial Intelligence and Statistics*, volume 54 of *Proceedings of Machine Learning Research*, pages 878–887. PMLR, 20–22 Apr 2017.
- [16] Beal, M. J. *Variational algorithms for approximate Bayesian inference*. University of London, University College London (United Kingdom), 2003.
- [17] Alaa, A. M. & Schaar, M.van der . Attentive state-space modeling of disease progression. *Advances in neural information processing systems*, 32, 2019.
- [18] Girin, L., Leglaive, S., Bie, X., Diard, J., Hueber, T. & Alameda-Pineda, X. Dynamical variational autoencoders: A comprehensive review. *arXiv preprint arXiv:2008.12595*, 2020.
- [19] Hafner, D., Lillicrap, T., Fischer, I., Villegas, R., Ha, D., Lee, H. & Davidson, J. Learning latent dynamics for planning from pixels. In *International conference on machine learning*, pages 2555–2565. PMLR, 2019.
- [20] Johnson, M. J., Duvenaud, D., Wiltchko, A. B., Datta, S. R. & Adams, R. P. Structured VAEs: Composing probabilistic graphical models and variational autoencoders. *arXiv preprint arXiv:1603.06277*, 2:2016, 2016.
- [21] Zhao, Y. & Linderman, S. Revisiting structured variational autoencoders. In *International Conference on Machine Learning*, pages 42046–42057. PMLR, 2023.

- [22] Khan, M. E. & Rue, H. The bayesian learning rule. *arXiv preprint arXiv:2107.04562*, 2021.
- [23] Hamelijnck, O., Wilkinson, W., Loppi, N., Solin, A. & Damoulas, T. Spatio-temporal variational Gaussian processes. In *Advances in Neural Information Processing Systems (NeurIPS)*, 2021.
- [24] Cseke, B. & Heskes, T. Approximate marginals in latent gaussian models. *The Journal of Machine Learning Research*, 12:417–454, 2011.
- [25] Botey, A., Jaegle, A., Wirnsberger, P., Hennes, D. & Higgins, I. Which priors matter? Benchmarking models for learning latent dynamics. *arXiv preprint arXiv:2111.05458*, 2021.
- [26] Jiang, X., Missel, R., Li, Z. & Wang, L. Sequential latent variable models for few-shot high-dimensional time-series forecasting. In *The Eleventh International Conference on Learning Representations*.
- [27] Missel, R. Torchneuralssm. <https://github.com/qu-gg/torchssm>, 2022.
- [28] Krishnan, R. G., Shalit, U. & Sontag, D. Deep kalman filters. *arXiv preprint arXiv:1511.05121*, 2015.
- [29] Churchland, M. M., Cunningham, J. P., Kaufman, M. T., Foster, J. D., Nuyujukian, P., Ryu, S. I. & Shenoy, K. V. Neural population dynamics during reaching. *Nature*, 487(7405):51–56, 2012.
- [30] Pei, F., Ye, J., Zoltowski, D. M., Wu, A., Chowdhury, R. H., Sohn, H., O’Doherty, J. E., Shenoy, K. V., Kaufman, M. T., Churchland, M., Jazayeri, M., Miller, L. E., Pillow, J., Park, I. M., Dyer, E. L. & Pandarinath, C. Neural latents benchmark ’21: evaluating latent variable models of neural population activity. In *Advances in Neural Information Processing Systems (NeurIPS), Track on Datasets and Benchmarks*, 2021.
- [31] Sohn, H., Narain, D. & Jazayeri, N. M. M. Bayesian computation through cortical latent dynamics. *Neuron*, 103(5):934–947, sep 2019.
- [32] Cong, Y., Chen, B. & Zhou, M. Fast simulation of hyperplane-truncated multivariate normal distributions. 2017.
- [33] Elfving, S., Uchibe, E. & Doya, K. Sigmoid-weighted linear units for neural network function approximation in reinforcement learning. *Neural Networks*, 107:3–11, 2018.
- [34] Jiang, X., Missel, R., Li, Z. & Wang, L. Sequential latent variable models for few-shot high-dimensional time-series forecasting. In *The Eleventh International Conference on Learning Representations*, 2023.

Contents

A Nomenclature	12
B Variational filtering	13
B.1 Variational predict step	13
B.2 Variational update step	13
B.3 Efficiently sampling structured marginals	14
C Evaluating the KL using low-rank structure	14
C.1 Smoothing inference network	14
C.2 Causal/streaming inference network	15
D Comparison method details	16
D.1 SVAE	16
D.2 DVBF	17
D.3 DKF	17
E Experimental details	17
E.1 High-dimensional linear dynamical system	17
E.2 Time complexity	17
E.3 Pendulum	17
E.4 Bouncing ball	18
E.5 MC_Maze	19
E.6 DMFC_RSG	19
F Useful expressions	20

A Nomenclature

Symbol	Description
SSM	state-space model
LGSSM	linear and Gaussian state-space model
$\pi(\mathbf{z}_t)$	variational approximation, $\pi(\mathbf{z}_t) \approx p(\mathbf{z}_t \mathbf{y}_{1:T})$
$\boldsymbol{\lambda}_t$	natural parameters of $\pi(\mathbf{z}_t)$
$\boldsymbol{\mu}_t$	mean parameters of $\pi(\mathbf{z}_t)$
$\mathbf{m}_t / \mathbf{P}_t$	mean / covariance of $\pi(\mathbf{z}_t)$
$\boldsymbol{\alpha}_t$	local natural parameter update, $\boldsymbol{\alpha}_\phi(\mathbf{y}_t)$
$\boldsymbol{\beta}_{t+1}$	backward natural parameter update, $\boldsymbol{\beta}_\phi(\mathbf{y}_{t+1:T})$
$\bar{\pi}(\mathbf{z}_t)$	variational approximation with mean parameters $\bar{\boldsymbol{\mu}}_t = \mathbb{E}_{\pi_{t-1}}[\boldsymbol{\mu}_\theta(\mathbf{z}_{t-1})]$
$\bar{\boldsymbol{\lambda}}_t$	natural parameters of $\bar{\pi}(\mathbf{z}_t)$
$\bar{\boldsymbol{\mu}}_t$	mean parameters of $\bar{\pi}(\mathbf{z}_t)$
$\bar{\mathbf{m}}_t / \bar{\mathbf{P}}_t$	mean / covariance of $\bar{\pi}(\mathbf{z}_t)$
$\boldsymbol{\theta}$	parameters of the dynamics and initial condition
$p_\theta(\mathbf{z}_t \mathbf{z}_{t-1})$	prior over state transitions
$p_\theta(\mathbf{z}_1)$	prior over initial condition
ψ	parameters of the observation model/likelihood
$p_\psi(\mathbf{y}_t \mathbf{z}_t)$	observation model/likelihood

B Variational filtering

Principles of Bayesian inference make it straightforward to write down an algorithm recursively computing the filtering posterior, $p(\mathbf{z}_t | \mathbf{y}_{1:t})^2$. Given, $p(\mathbf{z}_{t-1} | \mathbf{y}_{1:t-1})$, updating our belief to $p(\mathbf{z}_t | \mathbf{y}_{1:t})$ after observing \mathbf{y}_t can be broken down into two steps: first, we marginalize $p(\mathbf{z}_{t-1} | \mathbf{y}_{1:t-1})$ through the dynamics to obtain the predictive distribution,

$$\bar{p}(\mathbf{z}_t | \mathbf{y}_{1:t-1}) = \mathbb{E}_{p(\mathbf{z}_{t-1} | \mathbf{y}_{1:t-1})} [p_{\theta}(\mathbf{z}_t | \mathbf{z}_{t-1})] \quad \text{(predict step)} \quad (37)$$

Then, we update our belief by incorporating \mathbf{y}_t through Baye's rule,

$$p(\mathbf{z}_t | \mathbf{y}_{1:t}) \propto p_{\psi}(\mathbf{y}_t | \mathbf{z}_t) \bar{p}(\mathbf{z}_t | \mathbf{y}_{1:t-1}) \quad \text{(update step)} \quad (38)$$

However, these steps can usually not be evaluated in closed form when we depart from assumptions of Gaussianity and linearity. For nonlinear Gaussian dynamics the predict step can not be carried out exactly, and for nonlinear or non-Gaussian observations neither can the update step.

Alternatively, by considering variational analogues of the predict / update steps, we can develop a recursive and fully differentiable procedure for finding approximations $\pi(\mathbf{z}_t) \approx p(\mathbf{z}_t | \mathbf{y}_{1:t})$. In developing the variational analogues, it is assumed the approximations belong to an exponential family of distributions, (i.e. $\pi \in \mathcal{Q}$ where \mathcal{Q} is an exponential family distribution) – not necessarily Gaussian.

B.1 Variational predict step

Similar to developing a recursive algorithm as in the exact case, given $\pi(\mathbf{z}_{t-1}) \approx p(\mathbf{z}_{t-1} | \mathbf{y}_{1:t-1})$, we approximately marginalize $\pi(\mathbf{z}_{t-1})$ through the dynamics, by solving the following variational (forward KL / moment-matching) problem,

$$\bar{\pi}(\mathbf{z}_t) = \operatorname{argmin}_{\bar{\pi} \in \mathcal{Q}} \mathbb{D}_{\text{KL}}(\mathbb{E}_{\pi(\mathbf{z}_{t-1})} [p_{\theta}(\mathbf{z}_t | \mathbf{z}_{t-1})] || \bar{\pi}(\mathbf{z}_t)) \quad (39)$$

So that if $p_{\theta}(\mathbf{z}_t | \mathbf{z}_{t-1}) \in \mathcal{Q}$, the optimization problem is minimized when the mean parameters of $\bar{\pi}(\mathbf{z}_t)$, denoted $\bar{\boldsymbol{\mu}}_t$, are set to the expected mean parameter transformation under $\pi(\mathbf{z}_{t-1})$,

$$\bar{\boldsymbol{\mu}}_t = \mathbb{E}_{\pi(\mathbf{z}_{t-1})} [\boldsymbol{\mu}_{\theta}(\mathbf{z}_{t-1})] \quad \text{(variational predict step)} \quad (40)$$

For a LGSSM with $p_{\theta}(\mathbf{z}_t | \mathbf{z}_{t-1}) = \mathcal{N}(\mathbf{F}\mathbf{z}_{t-1}, \mathbf{Q})$, using the fact that,

$$\boldsymbol{\mu}_{\theta}(\mathbf{z}_{t-1}) = \left[\begin{array}{c} \mathbf{F}\mathbf{z}_{t-1} \\ -\frac{1}{2} (\mathbf{F}\mathbf{z}_{t-1}\mathbf{z}_{t-1}^{\top}\mathbf{F}^{\top} + \mathbf{Q}_{\theta}) \end{array} \right] \quad (41)$$

means that if $\pi(\mathbf{z}_{t-1}) = \mathcal{N}(\mathbf{m}_{t-1}, \mathbf{P}_{t-1})$, setting the mean and variance of $\bar{\pi}(\mathbf{z}_t)$ to,

$$\bar{\mathbf{m}}_t = \mathbf{F}\mathbf{m}_{t-1} \quad (42)$$

$$\bar{\mathbf{P}}_t = \mathbf{F}\mathbf{P}_{t-1}\mathbf{F}^{\top} + \mathbf{Q}_{\theta} \quad (43)$$

minimizes the forward KL objective, and reassuringly, recovers the familiar Kalman filter predict step.

B.2 Variational update step

For the variational analogue of the filtering update step, we use $\bar{\pi}(\mathbf{z}_t)$ as a prior for the latest observation, \mathbf{y}_t , and solve the following variational (reverse KL) problem,

$$\pi(\mathbf{z}_t) = \operatorname{argmin}_{\pi \in \mathcal{Q}} \mathbb{D}_{\text{KL}}(\pi(\mathbf{z}_t) || p_{\psi}(\mathbf{y}_t | \mathbf{z}_t) \bar{\pi}(\mathbf{z}_t)) \quad (44)$$

If we denote the natural parameters of $\pi(\mathbf{z}_t)$ by $\boldsymbol{\lambda}_t$, then the optimal $\boldsymbol{\lambda}_t$ satisfy the implicit equation²²,

$$\boldsymbol{\lambda}_t = \nabla_{\boldsymbol{\mu}_t} \mathbb{E}_{\pi_t} [\log p_{\psi}(\mathbf{y}_t | \mathbf{z}_t)] + \bar{\boldsymbol{\lambda}}_t \quad \text{(variational update step)} \quad (45)$$

This usually requires an iterative optimization procedure, except when the likelihood is conjugate to $\pi(\mathbf{z}_t)$ in which case, the likelihood must take the following form with respect to \mathbf{z}_t ,

$$p_{\psi}(\mathbf{y}_t | \mathbf{z}_t) \propto \exp(\mathcal{T}(\mathbf{z}_t)^{\top} \tilde{\boldsymbol{\lambda}}_t) \quad (46)$$

so that, as expected, the natural parameters of the solution are given as Baye’s rule would suggest – by adding the data dependent update to the natural parameters of the prior so that,

$$\boldsymbol{\lambda}_t = \tilde{\boldsymbol{\lambda}}_t + \bar{\boldsymbol{\lambda}}_t \quad (47)$$

For a LGSSM with $p_\psi(\mathbf{y}_t | \mathbf{z}_t) = \mathcal{N}(\mathbf{C}\mathbf{z}_t, \mathbf{R})$, this results in the following updates,

$$\mathbf{h}_t = \bar{\mathbf{h}}_t + \mathbf{C}^\top \mathbf{R}^{-1} \mathbf{y}_t \quad (48)$$

$$\mathbf{J}_t = \bar{\mathbf{J}}_t + \mathbf{C}^\top \mathbf{R}^{-1} \mathbf{C} \quad (49)$$

which reassuringly recover the information form of the Kalman filter update step¹⁶.

B.3 Efficiently sampling structured marginals

Algorithm 2 Nonlinear variational filtering

Input: $\mathbf{k}_{1:T}, \mathbf{K}_{1:T}$
for $t = 1$ **to** T **do**
 $\bar{\mathbf{m}}_t = S^{-1} \sum \mathbf{m}_\theta(\mathbf{z}_{t-1}^s)$
 $\bar{\mathbf{M}}_t^c = S^{-1/2} [\mathbf{m}_\theta(\mathbf{z}_{t-1}^1) - \bar{\mathbf{m}}_t \cdots \mathbf{m}_\theta(\mathbf{z}_{t-1}^S) - \bar{\mathbf{m}}_t]$
 $\bar{\boldsymbol{\Upsilon}}_t = \text{Cholesky}(\mathbf{I}_S + \bar{\mathbf{M}}_t^{c\top} \mathbf{Q}^{-1} \bar{\mathbf{M}}_t^c)^{-1}$
 $\bar{\mathbf{h}}_t = \bar{\mathbf{P}}_t^{-1} \bar{\mathbf{m}}_t$ # using $[\mathbf{Q}, \bar{\mathbf{M}}_t^c, \bar{\boldsymbol{\Upsilon}}_t]$ and Eq. (30)
 $\boldsymbol{\Upsilon}_t = \text{Cholesky}(\mathbf{I}_r + \mathbf{K}_t^\top \bar{\mathbf{P}}_t \mathbf{K}_t)^{-1}$ # using $[\mathbf{Q}, \bar{\mathbf{M}}_t^c]$ and Eq. (29)
 $\mathbf{h}_t = \bar{\mathbf{h}}_t + \mathbf{k}_t$
 $\mathbf{m}_t = \mathbf{P}_t \mathbf{h}_t$ # using $[\mathbf{Q}, \bar{\mathbf{M}}_t^c, \mathbf{K}_t, \boldsymbol{\Upsilon}_t]$ and Eqs. (32) and (29)
 $\bar{\mathbf{w}}_t^s \sim \mathcal{N}(\mathbf{0}, \mathbf{I}_{L+S})$
 $\bar{\mathbf{z}}_t^s = \bar{\mathbf{P}}_t^{1/2} \bar{\mathbf{w}}_t^s$ # using $[\mathbf{Q}, \bar{\mathbf{M}}_t^c]$ and Eq. (29)
 $\mathbf{w}_t^s \sim \mathcal{N}(\mathbf{0}, \mathbf{I}_r)$
 $\mathbf{z}_t^s = \mathbf{m}_t + \bar{\mathbf{z}}_t^s - \mathbf{K}_t \boldsymbol{\Upsilon}_t \boldsymbol{\Upsilon}_t^\top (\mathbf{K}_t^\top \bar{\mathbf{z}}_t^s + \mathbf{w}_t^s)$
end for
Output: $\mathbf{z}_{1:T}^s, \mathbf{m}_{1:T}, \bar{\mathbf{m}}_{1:T}, \boldsymbol{\Upsilon}_{1:T}$

While \mathbf{P}_t has a structured representation, drawing samples from $\pi(\mathbf{z}_t)$ is not straightforward because we do not have a structured representation for a square-root of \mathbf{P}_t . However, using the factorization of $\bar{\mathbf{P}}_t$ in Eq. (29), it is possible to sample from $\mathcal{N}(\mathbf{0}, \bar{\mathbf{P}}_t)$ efficiently since $\bar{\mathbf{P}}_t^{1/2} = [\bar{\mathbf{M}}_t^c \mathbf{Q}^{1/2}]$. Now, combining the fact that the posterior marginal can be written as,

$$\begin{aligned} \pi(\mathbf{z}_t) &= \mathcal{N}(\mathbf{m}_t, \mathbf{P}_t) \\ &= \mathcal{N}(\mathbf{m}_t, (\bar{\mathbf{P}}_t^{-1} + \mathbf{K}_t \mathbf{K}_t^\top)^{-1}) \end{aligned} \quad (50)$$

with the result from Cong et al.³², stating that sampling $\mathbf{z}_t^s \sim \pi(\mathbf{z}_t)$ is equivalent to sampling $\mathbf{w}_t^s \sim \mathcal{N}(\mathbf{0}, \mathbf{I}_{L+S})$ and $\bar{\mathbf{z}}_t^s \sim \mathcal{N}(\mathbf{0}, \bar{\mathbf{P}}_t)$, and then setting

$$\mathbf{z}_t^s = \mathbf{m}_t + \bar{\mathbf{z}}_t^s - \mathbf{K}_t \boldsymbol{\Upsilon}_t \boldsymbol{\Upsilon}_t^\top (\mathbf{K}_t^\top \bar{\mathbf{z}}_t^s + \mathbf{w}_t^s), \quad (51)$$

makes it possible to efficiently draw samples from the posterior marginal.

C Evaluating the KL using low-rank structure

C.1 Smoothing inference network

Efficient training of the generative model and inference networks require efficient numerical evaluation of the ELBO. We take advantage of the structured precision matrices arising from low-rank updates and sample approximations. The expected log likelihood can be evaluated using a Monte Carlo approximation from samples during the filtering pass. The KL term,

$$\mathbb{D}_{\text{KL}}(\pi(\mathbf{z}_t) || \bar{\pi}(\mathbf{z}_t)) = \frac{1}{2} \left[(\bar{\mathbf{m}}_t - \mathbf{m}_t)^\top \bar{\mathbf{P}}_t^{-1} (\bar{\mathbf{m}}_t - \mathbf{m}_t) + \text{tr}(\bar{\mathbf{P}}_t^{-1} \mathbf{P}_t) + \log \frac{|\bar{\mathbf{P}}_t|}{|\mathbf{P}_t|} - L \right] \quad (52)$$

can be evaluated in closed form and we can expand each term as,

Log-determinant. Writing

$$\log |\mathbf{P}_t| = -\log |\bar{\mathbf{P}}_t^{-1} + \mathbf{K}_t \mathbf{K}_t^\top| \quad (53)$$

$$= \log |\bar{\mathbf{P}}_t| - \log |\mathbf{I} + \mathbf{K}_t^\top \bar{\mathbf{P}}_t \mathbf{K}_t| \quad (54)$$

gives

$$\log \frac{|\bar{\mathbf{P}}_t|}{|\mathbf{P}_t|} = \log |\mathbf{I} + \mathbf{K}_t^\top \bar{\mathbf{P}}_t \mathbf{K}_t| \quad (55)$$

$$= -2 \sum_{i=1}^r [\boldsymbol{\Upsilon}_t]_{i,i} \quad (56)$$

Trace. Writing,

$$\text{tr}(\bar{\mathbf{P}}_t^{-1} \mathbf{P}_t) = \text{tr}(\mathbf{I}_L - \mathbf{K}_t (\mathbf{I} + \mathbf{K}_t^\top \bar{\mathbf{P}}_t \mathbf{K}_t)^{-1} \mathbf{K}_t^\top \bar{\mathbf{P}}_t) \quad (57)$$

$$= L - \text{tr}(\bar{\mathbf{P}}_t^{\top/2} \mathbf{K}_t (\mathbf{I} + \mathbf{K}_t^\top \bar{\mathbf{P}}_t \mathbf{K}_t)^{-1} \mathbf{K}_t^\top \bar{\mathbf{P}}_t^{1/2}) \quad (58)$$

$$= L - \text{tr}(\boldsymbol{\Upsilon}_t^\top \mathbf{K}_t^\top \bar{\mathbf{P}}_t \mathbf{K}_t \boldsymbol{\Upsilon}_t) \quad (59)$$

which by taking $\boldsymbol{\Upsilon}_t$ to be an $r \times r$ square root such that,

$$\boldsymbol{\Upsilon}_t \boldsymbol{\Upsilon}_t^\top = (\mathbf{I} + \mathbf{K}_t^\top \bar{\mathbf{P}}_t \mathbf{K}_t)^{-1} \quad (60)$$

further simplifies to

$$\text{tr}(\bar{\mathbf{P}}_t^{-1} \mathbf{P}_t) = L - \text{tr}(\bar{\mathbf{M}}_t^{c\top} \mathbf{K}_t \boldsymbol{\Upsilon}_t \boldsymbol{\Upsilon}_t^\top \mathbf{K}_t^\top \bar{\mathbf{M}}_t^c) - \text{tr}(\mathbf{Q}^{\top/2} \mathbf{K}_t \boldsymbol{\Upsilon}_t \boldsymbol{\Upsilon}_t^\top \mathbf{K}_t^\top \mathbf{Q}^{1/2}) \quad (61)$$

$$= L - \text{tr}(\bar{\mathbf{M}}_t^{c\top} \mathbf{K}_t \boldsymbol{\Upsilon}_t \boldsymbol{\Upsilon}_t^\top \mathbf{K}_t^\top \bar{\mathbf{M}}_t^c) - \text{tr}(\boldsymbol{\Upsilon}_t^\top \mathbf{K}_t^\top \mathbf{Q}^{1/2} \mathbf{Q}^{\top/2} \mathbf{K}_t \boldsymbol{\Upsilon}_t) \quad (62)$$

note that the size of the triple product, $\bar{\mathbf{M}}_t^{c\top} \mathbf{K}_t \boldsymbol{\Upsilon}_t$, is $S \times r$.

C.2 Causal/streaming inference network

When the real-time parameterization of the inference network is used the expressions become slightly more complicated due to the more intricate relationship between the posterior at time t and the posterior predictive at time t .

Log-determinant. We need to first find $\log |\bar{\mathbf{P}}_{t|T}| - \log |\mathbf{P}_t|$ so begin with using the matrix-determinant lemma to write,

$$|\bar{\mathbf{P}}_{t|T}| = |\mathbf{M}_{t|T}^c \mathbf{M}_{t|T}^{c\top} + \mathbf{Q}| \quad (63)$$

$$= |\mathbf{I}_S + \mathbf{M}_{t|T}^{c\top} \mathbf{Q}^{-1} \mathbf{M}_{t|T}^c| \times |\mathbf{Q}| \quad (64)$$

then expand the smoothed covariance to write,

$$|\mathbf{P}_t| = |(\check{\mathbf{P}}_t^{-1} + \mathbf{B}_t \mathbf{B}_t^\top)^{-1}| \quad (65)$$

$$= |\check{\mathbf{P}}_t^{-1} + \mathbf{B}_t \mathbf{B}_t^\top|^{-1} \quad (66)$$

$$= (|\mathbf{I}_{r_\beta} + \mathbf{B}_t^\top \check{\mathbf{P}}_t \mathbf{B}_t| \times |\check{\mathbf{P}}_t^{-1}|)^{-1} \quad (67)$$

$$= |\mathbf{I}_{r_\beta} + \mathbf{B}_t^\top \check{\mathbf{P}}_t \mathbf{B}_t|^{-1} |\check{\mathbf{P}}_t| \quad (68)$$

and another time to write,

$$|\check{\mathbf{P}}_t^{-1}| = |\bar{\mathbf{P}}_t^{-1} + \mathbf{A}_t \mathbf{A}_t^\top| \quad (69)$$

$$= |\mathbf{I}_{r_\alpha} + \mathbf{A}_t^\top \bar{\mathbf{P}}_t \mathbf{A}_t| \times |\bar{\mathbf{P}}_t^{-1}| \quad (70)$$

and another time,

$$|\bar{\mathbf{P}}_t| = |\mathbf{M}_t^c \mathbf{M}_t^{c\top} + \mathbf{Q}| \quad (71)$$

$$= |\mathbf{I}_S + \mathbf{M}_t^{c\top} \mathbf{Q}^{-1} \mathbf{M}_t^c| \times |\mathbf{Q}| \quad (72)$$

When combined we are finally able to write

$$\log |\bar{\mathbf{P}}_{t|T}| - \log |\mathbf{P}_t| = \log |\mathbf{I}_S + \mathbf{M}_{t|T}^{c\top} \mathbf{Q}^{-1} \mathbf{M}_{t|T}^c| + \log |\mathbf{I}_{r_\beta} + \mathbf{B}_t^\top \check{\mathbf{P}}_t \mathbf{B}_t| \quad (73)$$

$$+ \log |\mathbf{I}_{r_\alpha} + \mathbf{A}_t^\top \bar{\mathbf{P}}_t \mathbf{A}_t| - \log |\mathbf{I}_S + \mathbf{M}_t^{c\top} \mathbf{Q}^{-1} \mathbf{M}_t^c| \quad (74)$$

For the initial condition we have,

$$\log |\bar{\mathbf{P}}_1| - \log |\mathbf{P}_1| = \log |\mathbf{I}_{r_\beta} + \mathbf{B}_1^\top \check{\mathbf{P}}_1 \mathbf{B}_1| + \log |\mathbf{I}_{r_\alpha} + \mathbf{A}_1^\top \bar{\mathbf{P}}_1 \mathbf{A}_1| \quad (75)$$

Trace. For the trace,

$$\text{tr}(\bar{\mathbf{P}}_{t|T}^{-1} \mathbf{P}_t) = \text{tr}(\mathbf{Q}^{-1} \mathbf{P}_t) - \text{tr}(\mathbf{Q}^{-1} \mathbf{M}_{t|T}^c (\mathbf{I}_S + \mathbf{M}_{t|T}^{c\top} \mathbf{Q}^{-1} \mathbf{M}_{t|T}^c)^{-1} \mathbf{M}_{t|T}^{c\top} \mathbf{Q}^{-1} \mathbf{P}_t) \quad (76)$$

$$= \text{tr}(\mathbf{Q}^{-1} \mathbf{P}_t) - \text{tr}(\mathbf{Q}^{-1} \mathbf{M}_{t|T}^c \bar{\mathbf{\Upsilon}}_{t|T} \bar{\mathbf{\Upsilon}}_{t|T}^\top \mathbf{M}_{t|T}^{c\top} \mathbf{Q}^{-1} \mathbf{P}_t) \quad (77)$$

$$= \text{tr}(\mathbf{P}_t \mathbf{Q}^{-1}) - \text{tr}([\mathbf{P}_t \mathbf{Q}^{-1} \mathbf{M}_{t|T}^c \bar{\mathbf{\Upsilon}}_{t|T}] \bar{\mathbf{\Upsilon}}_{t|T}^\top \mathbf{M}_{t|T}^{c\top} \mathbf{Q}^{-1}) \quad (78)$$

where we expand the first rhs term for a numerically efficient implementation by writing

$$\text{tr}(\mathbf{P}_t \mathbf{Q}^{-1}) = \text{tr}(\bar{\mathbf{P}}_t \mathbf{Q}^{-1}) - \text{tr}(\bar{\mathbf{P}}_t \mathbf{A}_t (\mathbf{I}_{r_\alpha} + \mathbf{A}_t^\top \bar{\mathbf{P}}_t \mathbf{A}_t)^{-1} \mathbf{A}_t^\top \bar{\mathbf{P}}_t \mathbf{Q}^{-1}) \quad (79)$$

$$- \text{tr}(\check{\mathbf{P}}_t \mathbf{B}_t (\mathbf{I}_{r_\beta} + \mathbf{B}_t^\top \check{\mathbf{P}}_t \mathbf{B}_t)^{-1} \mathbf{B}_t^\top \check{\mathbf{P}}_t \mathbf{Q}^{-1}) \quad (80)$$

To reduce notational clutter we define,

$$\bar{\mathbf{\Upsilon}}_t \bar{\mathbf{\Upsilon}}_t^\top = (\mathbf{I}_S + \mathbf{M}_t^{c\top} \mathbf{Q}^{-1} \mathbf{M}_t^c)^{-1} \quad (81)$$

$$\bar{\mathbf{\Upsilon}}_{t|T} \bar{\mathbf{\Upsilon}}_{t|T}^\top = (\mathbf{I}_S + \mathbf{M}_{t|T}^{c\top} \mathbf{Q}^{-1} \mathbf{M}_{t|T}^c)^{-1} \quad (82)$$

$$\check{\mathbf{\Upsilon}}_t \check{\mathbf{\Upsilon}}_t^\top = (\mathbf{I}_{r_\alpha} + \mathbf{A}_t^\top \bar{\mathbf{P}}_t \mathbf{A}_t)^{-1} \quad (83)$$

$$\mathbf{\Upsilon}_t \mathbf{\Upsilon}_t^\top = (\mathbf{I}_{r_\beta} + \mathbf{B}_t^\top \bar{\mathbf{P}}_t \mathbf{B}_t)^{-1} \quad (84)$$

and so the trace is

$$\text{tr}(\bar{\mathbf{P}}_{t|T}^{-1} \mathbf{P}_t) = L + \text{tr}(\mathbf{M}_t^{c\top} \mathbf{Q}^{-1} \mathbf{M}_t^c) - \text{tr}(\mathbf{Q}^{-1/2} \bar{\mathbf{P}}_t \mathbf{A}_t \check{\mathbf{\Upsilon}}_t \check{\mathbf{\Upsilon}}_t^\top \mathbf{A}_t^\top \bar{\mathbf{P}}_t \mathbf{Q}^{-1/2}) \quad (85)$$

$$- \text{tr}(\mathbf{Q}^{-1/2} \check{\mathbf{P}}_t \mathbf{B}_t \mathbf{\Upsilon}_t \mathbf{\Upsilon}_t^\top \mathbf{B}_t^\top \check{\mathbf{P}}_t \mathbf{Q}^{-1/2}) \quad (86)$$

$$- \text{tr}([\mathbf{P}_t \mathbf{Q}^{-1} \mathbf{M}_{t|T}^c \bar{\mathbf{\Upsilon}}_{t|T}] \bar{\mathbf{\Upsilon}}_{t|T}^\top \mathbf{M}_{t|T}^{c\top} \mathbf{Q}^{-1}) \quad (87)$$

which is now in a form that is easy to handle using fast MVMs with $\bar{\mathbf{P}}_t, \check{\mathbf{P}}_t, \mathbf{P}_t$.

For the initial condition term we use the fact that $\bar{\mathbf{P}}_1$ is diagonal,

$$\text{tr}(\mathbf{P}_1 \bar{\mathbf{P}}_1^{-1}) = L - \text{tr}(\bar{\mathbf{P}}_1^{1/2} \mathbf{A}_1 \check{\mathbf{\Upsilon}}_1 \check{\mathbf{\Upsilon}}_1^\top \mathbf{A}_1^\top \bar{\mathbf{P}}_1^{1/2}) - \text{tr}(\bar{\mathbf{P}}_1^{-1/2} \check{\mathbf{P}}_1 \mathbf{B}_1 \mathbf{\Upsilon}_1 \mathbf{\Upsilon}_1^\top \mathbf{B}_1^\top \check{\mathbf{P}}_1 \bar{\mathbf{P}}_1^{-1/2}) \quad (88)$$

D Comparison method details

D.1 SVAE

For the SVAE²⁰, the latent state prior is a linear dynamical system parameterized as,

$$p_\theta(\mathbf{z}_t | \mathbf{z}_{t-1}) = \mathcal{N}(\mathbf{z}_t | \mathbf{F} \mathbf{z}_{t-1}, \mathbf{Q}) \quad (89)$$

Using conjugate potentials, with likelihood $p(\tilde{\mathbf{y}}_t | \mathbf{z}_t) = \exp(t(\mathbf{z}_t)^\top \boldsymbol{\alpha}(\mathbf{y}_t))$, the approximate posterior is given by $q(\mathbf{z}_{1:T}) = \prod p(\tilde{\mathbf{y}}_t | \mathbf{z}_t) p_\theta(\mathbf{z}_{1:T})$ so that its statistics can be found by applying Kalman filtering/smoothing to the pseudo-observations. In this case, the ELBO can be evaluated as

$$\mathcal{L}(q) = \sum \mathbb{E}_{q_t} [\log p(\mathbf{y}_t | \mathbf{z}_t)] - \mathbb{E}_{q_t} [\log p(\tilde{\mathbf{y}}_t | \mathbf{z}_t)] + \log \mathbb{E}_{\bar{q}_t} [p(\tilde{\mathbf{y}}_t | \mathbf{z}_t)] \quad (90)$$

where $\bar{q}_t := \bar{q}(\mathbf{z}_t) = p(\mathbf{z}_t | \tilde{\mathbf{y}}_{1:t-1})$ is the filtering predictive distribution. These expressions can be evaluated in closed form and written concisely in terms of natural/mean parameters and log-partition functions as

$$\mathcal{L}(q) = \sum \mathbb{E}_{q_t} [\log p(\mathbf{y}_t | \mathbf{z}_t)] - \boldsymbol{\mu}_t^\top \boldsymbol{\alpha}_t + A(\bar{\boldsymbol{\lambda}}_t + \boldsymbol{\alpha}_t) - A(\bar{\boldsymbol{\lambda}}_t) \quad (91)$$

where $\boldsymbol{\mu}_t = \nabla A(\bar{\boldsymbol{\lambda}}_t + \boldsymbol{\alpha}_t + \boldsymbol{\beta}_{t+1})$. Using the identities given in App. F, these expressions can be written in more familiar mean/covariance parameters.

D.2 DVBF

For the DVBF⁵, we parameterize the latent state prior using a nonlinear dynamical system of the same form as Eq. (1). Then, using an inference network that encodes data in reverse-time to produce the parameters of a diagonal Gaussian distribution, $\mathbf{w}_t \sim q(\mathbf{w}_t) = \mathcal{N}(\mathbf{m}_t, \text{diag}(\mathbf{s}_t))$, we sample the latent trajectory forward using the recursion, $\mathbf{z}_t = \mathbf{m}_\theta(\mathbf{z}_{t-1}) + \mathbf{Q}^{1/2}\mathbf{w}_t$. Parameters of the generative model/inference network are learned jointly by minimizing the ELBO,

$$\mathcal{L}(q) = \sum \mathbb{E}_{q(\mathbf{z}_t)} [\log p_\psi(\mathbf{y}_t | \mathbf{z}_t)] - \mathbb{D}_{\text{KL}}(q(\mathbf{w}_t) || p(\mathbf{w}_t)) \quad (92)$$

where, $p(\mathbf{w}_t) = \mathcal{N}(\mathbf{0}, \mathbf{I})$.

D.3 DKF

For the DKF⁶, the latent state is also parameterized using a nonlinear dynamical system of the same form as Eq. (1). We follow the parameterization outlined in the text with S2S(\cdot) implemented using a recurrent neural network. We sample trajectories using the inference network and jointly train all parameters on the ELBO,

$$\mathcal{L}(q) = \sum \mathbb{E}_{q_t} [\log p(\mathbf{y}_t | \mathbf{z}_t)] - \mathbb{E}_{q_{t-1}} [\mathbb{D}_{\text{KL}}(q(\mathbf{z}_t | \mathbf{z}_{t-1}) || p_\theta(\mathbf{z}_t | \mathbf{z}_{t-1}))] \leq \log p(\mathbf{y}_{1:T}) \quad (93)$$

E Experimental details

In describing the neural network architectures used to parameterize the inference model, it will be useful to define the following multilayer perceptron (MLP), with SiLU nonlinearity³³, that gets used repeatedly:

$$- \text{MLP}(n_{\text{in}}, n_{\text{hidden}}, n_{\text{out}}) : [\text{Linear}(n_{\text{in}}, n_{\text{hidden}}), \text{SiLU}(), \text{Linear}(n_{\text{hidden}}, n_{\text{out}})]$$

$$\mathcal{L}(q) = \sum \mathbb{E}_{q_t} [\log p(\mathbf{y}_t | \mathbf{z}_t)] - \mathbb{E}_{q_{t-1}} [\mathbb{D}_{\text{KL}}(q(\mathbf{z}_t | \mathbf{z}_{t-1}) || p_\theta(\mathbf{z}_t | \mathbf{z}_{t-1}))] \leq \log p(\mathbf{y}_{1:T}) \quad (94)$$

E.1 High-dimensional linear dynamical system

We simulated data from an LDS generative model (with dynamics restricted to the set of matrices with singular values less than 1) for latent dimensions $L \in [20, 50, 100]$ over 3 random seeds for two scenarios **i**) $N = L$ and **ii**) $N = L/5$. For each scenario, we also vary the rank of the local/backward encoder precision updates.

E.2 Time complexity

We generate random LDS systems of appropriate dimension and measure the average time to complete one forward pass and take a gradient step. The system used for benchmarking wall-clock time was an RTX 4090 with 128GB of RAM with an AMD 5975WX processor.

E.3 Pendulum

We consider the pendulum system from²⁵. We generate 500/150/150 trials of length 100 for training/validation/testing. All methods are trained for 5000 epochs for 3 different random seeds. We consider a context window of 50 images and a forecast window of 50 images. A decoder was fit from the latent state on the training set during the context window; then, for held out data, we examine performance of the decoder during the context and forecast windows.

The generative model is parameterized as:

- $L = 4$
- $N = 256$
- $T = 50$
- likelihood

- $p_{\psi}(\mathbf{y}_t | \mathbf{z}_t) = \mathcal{N}(\mathbf{z}_t | \mathbf{C}_{\psi}(\mathbf{z}_t) + \mathbf{b}, \mathbf{R})$
- \mathbf{C}_{ψ} : MLP(4, 128, 256)

For each method, inference is amortized using the following neural network architectures:

- our inference network
 - $r_{\alpha} = 4$
 - $r_{\beta} = 4$
 - α_{ϕ} : MLP(256, 128, 20)
 - β_{ϕ} : [GRU(128), Linear(128, 20)]
- DKF inference network
 - \mathbf{u}_{ϕ} : GRU(128)
 - $(\mathbf{m}_{\phi}, \log \mathbf{P}_{\phi})$: MLP(132, 128, 8)
- DVBF inference network
 - \mathbf{u}_{ϕ} : [GRU(128)]
 - $(\boldsymbol{\mu}_{\phi}, \log \boldsymbol{\sigma}_{\phi})$: MLP(132, 128, 8)
- SVAE inference network
 - α_{ϕ} : MLP(256, 128, 20)

Optimization and training details:

- optimizer: Adam(lr = 0.001)
- batch size: 128

E.4 Bouncing ball

We consider a bouncing ball dataset commonly used as a baseline to benchmark the performance of inference and learning in deep state-space models^{25,34,34}. For this dataset we take 500/150/150 trials of length 75 for training/validation/testing. All methods are trained for 5000 epochs for 3 different random seeds. The generative model is parameterized as:

- $L = 8$
- $N = 256$
- $T = 50$
- likelihood
 - $p_{\psi}(\mathbf{y}_t | \mathbf{z}_t) = \mathcal{N}(\mathbf{z}_t | \mathbf{C}_{\psi}(\mathbf{z}_t) + \mathbf{b}, \mathbf{R})$
 - \mathbf{C}_{ψ} : MLP(8, 128, 256)

For each method, inference is amortized using the following neural network architectures:

- our inference network
 - $r_{\alpha} = 8$
 - $r_{\beta} = 4$
 - α_{ϕ} : MLP(256, 128, 72)
 - β_{ϕ} : [GRU(128), Linear(128, 40)]
- DKF inference network
 - \mathbf{u}_{ϕ} : GRU(128)
 - $(\mathbf{m}_{\phi}, \log \mathbf{P}_{\phi})$: MLP(132, 128, 16)
- DVBF inference network
 - \mathbf{u}_{ϕ} : [GRU(128)]
 - $(\boldsymbol{\mu}_{\phi}, \log \boldsymbol{\sigma}_{\phi})$: MLP(132, 128, 16)
- SVAE inference network

- α_ϕ : MLP(256, 128, 72)

Optimization and training details:

- optimizer: Adam(lr = 0.001)
- batch size: 128

E.5 MC_Maze

The monkey reaching dataset of²⁹ was the first real dataset examined in the main text. For this dataset, we partitioned 1800/200/200 training/validation/testing trials sampled at 20ms per bin. All methods are trained for 1000 epochs for 3 different random seeds. The generative model is parameterized as:

- $L = 40$
- $N = 182$
- $T = 35$
- likelihood
 - $p_\psi(\mathbf{y}_t | \mathbf{z}_t) = \text{Poisson}(\mathbf{z}_t | \mathbf{C}_\psi(\mathbf{z}_t) + \mathbf{b})$
 - \mathbf{C}_ψ : Linear(40, 182)

For each method, inference is amortized using the following neural network architectures:

- our inference network
 - $r_\alpha = 15$
 - $r_\beta = 5$
 - α_ϕ : MLP(182, 128, 640)
 - β_ϕ : [GRU(128), Linear(128, 240)]
- DKF inference network
 - \mathbf{u}_ϕ : GRU(128)
 - $(\mathbf{m}_\phi, \log \mathbf{P}_\phi)$: MLP(128, 128, 80)
- DVBF inference network
 - \mathbf{u}_ϕ : [GRU(128)]
 - $(\mathbf{m}_\phi, \log \mathbf{P}_\phi)$: MLP(128, 128, 80)
- SVAE inference network
 - α_ϕ : MLP(182, 256, 1640)

Optimization and training details:

- optimizer: Adam(lr = 0.001)
- batch size: 128

E.6 DMFC_RSG

The second real dataset examined was the timing interval reproduction task of³¹ samples at 10ms bins. For this dataset, we partitioned 700/150/150 training/validation/testing trials. All methods are trained for 1000 epochs for 3 different random seeds. The generative model is parameterized as:

- $L = 40$
- $N = 54$
- $T = 130$
- likelihood
 - $p_\psi(\mathbf{y}_t | \mathbf{z}_t) = \text{Poisson}(\mathbf{z}_t | \mathbf{C}_\psi(\mathbf{z}_t) + \mathbf{b})$
 - \mathbf{C}_ψ : Linear(40, 54)

For each method, inference is amortized using the following neural network architectures:

- our inference network
 - $r_\alpha = 15$
 - $r_\beta = 5$
 - α_ϕ : MLP(54, 128, 640)
 - β_ϕ : [GRU(128), Linear(128, 240)]
- DKF inference network
 - \mathbf{u}_ϕ : GRU(128)
 - $(\mathbf{m}_\phi, \log \mathbf{P}_\phi)$: MLP(128, 128, 80)
- DVBF inference network
 - \mathbf{u}_ϕ : [GRU(128)]
 - $(\boldsymbol{\mu}_\phi, \log \boldsymbol{\sigma}_\phi)$: MLP(128, 128, 80)
- SVAE inference network
 - α_ϕ : MLP(256, 128, 1640)

Optimization and training details:

- optimizer: Adam(lr = 0.001)
- batch size: 128

F Useful expressions

mean/natural parameter inner product One common expression that frequently arises is the inner product between a mean and natural parameter, i.e.

$$\boldsymbol{\mu}_t^\top \boldsymbol{\alpha}_t \tag{95}$$

where in the Gaussian case if the mean/natural parameter coordinates are,

$$\boldsymbol{\mu}_t = \left(-\frac{1}{2}(\mathbf{P}_t + \mathbf{m}_t \mathbf{m}_t^\top) \right) \quad \boldsymbol{\alpha}_t = \left(\begin{array}{c} \mathbf{a}_t \\ \mathbf{A}_t \mathbf{A}_t^\top \end{array} \right) \tag{96}$$

then,

$$\boldsymbol{\mu}_t^\top \boldsymbol{\alpha}_t = \mathbf{m}_t^\top \mathbf{a}_t - \frac{1}{2} \|\mathbf{A}_t^\top \mathbf{m}_t\|^2 - \frac{1}{2} \text{tr}(\mathbf{A}_t^\top \mathbf{P}_t \mathbf{A}_t) \tag{97}$$

difference of log partition functions Another common expression that frequently arises is given by,

$$A(\bar{\boldsymbol{\lambda}}_t + \boldsymbol{\alpha}_t) - A(\bar{\boldsymbol{\lambda}}_t) \tag{98}$$

so that if,

$$\bar{\boldsymbol{\lambda}}_t = \left(\begin{array}{c} \bar{\mathbf{P}}_t^{-1} \bar{\mathbf{m}}_t \\ \bar{\mathbf{P}}_t^{-1} \end{array} \right) \tag{99}$$

then,

$$A(\bar{\boldsymbol{\lambda}}_t + \boldsymbol{\alpha}_t) - A(\bar{\boldsymbol{\lambda}}_t) \tag{100}$$

$$= \frac{1}{2} \check{\mathbf{m}}_t^\top (\bar{\mathbf{P}}_t^{-1} + \mathbf{A}_t \mathbf{A}_t^\top) \check{\mathbf{m}}_t - \frac{1}{2} \log |\bar{\mathbf{P}}_t^{-1} + \mathbf{A}_t \mathbf{A}_t^\top| \tag{101}$$

$$- \frac{1}{2} \bar{\mathbf{m}}_t \bar{\mathbf{P}}_t^{-1} \bar{\mathbf{m}}_t + \frac{1}{2} \log |\bar{\mathbf{P}}_t^{-1}|$$

$$= \frac{1}{2} \left(\|\check{\mathbf{m}}_t\|_{\bar{\mathbf{P}}_t^{-1}}^2 - \|\bar{\mathbf{m}}_t\|_{\bar{\mathbf{P}}_t^{-1}}^2 + \|\mathbf{A}_t^\top \check{\mathbf{m}}_t\|^2 - \log |\mathbf{I} + \mathbf{A}_t^\top \bar{\mathbf{P}}_t \mathbf{A}_t| \right) \tag{102}$$